**WSRC-MS-2000-00747**

# Tritium and Decay Helium Effects on Cracking Thresholds and Velocities in Stainless Steel (U)

Michael J. Morgan
Westinghouse Savannah River Company
Savannah River Technology Center
Aiken, SC 29808
803-725-2245
803-725-7369 (Fax)
michael.morgan@srs.gov

And

Michael H. Tosten
Westinghouse Savannah River Company
Savannah River Technology Center
Aiken, SC 29808
803-725-3592
Michael.tosten@srs.gov

*A paper for publication in the conference proceedings of the*

14th ANS Topical Meeting on the Technology of Fusion Energy
Park City, Utah

This document was prepared in conjunction with work accomplished under Contract No. DE-AC09-96SR18500 with the U.S. Department of Energy.

**DISCLAIMER**

# TRITIUM AND DECAY HELIUM EFFECTS ON CRACKING THRESHOLDS AND VELOCITIES IN STAINLESS STEEL*

Michael J. Morgan
Westinghouse Savannah River Company
Savannah River Technology Center
Aiken, SC 29808
803-725-2245

Michael H. Tosten
Westinghouse Savannah River Company
Savannah River Technology Center
Aiken, SC 29808
803-725-3592

## ABSTRACT

Crack initiation and propagation were studied in three tritium-exposed stainless steels. The purpose was to measure cracking thresholds and velocities as a function of helium concentration in Type 21-6-9 stainless steel and compare the results to earlier measurements on Types 316L and 304L steels. Fracture toughness specimens were cut from forgings, fatigue-cracked and exposed to tritium at 423 K and 31 MPa. The samples were aged for selected times at 273 K to "build-in" $^3$He from tritium decay. Tritium concentrations ranged from 0-2600 atomic parts per million (appm) and $^3$He concentrations ranged from 0-600 appm. The samples were step-loaded at room temperature in air using a screw-driven mechanical testing machine and held at fixed displacement until crack initiation was detected. Crack propagation was monitored by continuously recording the drop in load until crack arrest. Threshold stress intensity was calculated from the load and the crack length at the end of the test. Crack velocities were determined from the load-time records and compliance relationships and verified on some samples using a DC potential-drop technique. The crack path was along grain and twin boundaries. For 21-6-9, the threshold for cracking decreased with increasing helium concentrations from about 90 MPa-m$^{1/2}$ (50 appm helium) to 25 MPa-m$^{1/2}$ (600 appm helium). Steady-state-crack velocities averaged $10^{-7}$ m/s and was not strongly dependent on helium concentration. The data show that embrittlement of tritium-exposed is a form of hydrogen embrittlement made worse by the hardening of the microstructure from nanometer-sized helium bubbles that build-in with tritium decay.

## I. INTRODUCTION

Tritium containment systems are an important aspect of fusion technology. Austenitic stainless steels are generally chosen for these applications because of the high resistance to the embrittling effects of hydrogen. Types 304L, 316L and 21-6-9 stainless steels are all used as materials of construction for tritium containment at the Savannah River Site. Type 21-6-9 stainless steel is used mainly to take advantage of its higher strength than the other steels. Like all austenitic stainless steels, it is highly resistant to, but not immune from, embrittlement by hydrogen and its isotopes. This material's yield strength, nitrogen content (1) and microstructure (2-4) affect the degree to which it is affected by hydrogen isotopes. For steels exposed to tritium for extended periods of time, hydrogen-induced cracking can be more of a problem because of the build-in of helium from tritium dissolution, diffusion, and radioactive decay (4-6). At ambient temperatures, $^3$He enhances the embrittlement from hydrogen by hardening the microstructure as nanometer-sized helium bubbles build-in from tritium decay. Helium bubbles enhance embrittlement by trapping hydrogen in their large strain fields, pinning dislocations and creating obstacles to dislocation motion (2,4, 7).

In this study, crack initiation and propagation was studied in tritium-exposed Type 21-6-9 stainless steel. The goal of the study was to measure the threshold stress intensity for cracking and crack growth rates as a function of helium concentration and to compare the results to those measured in an earlier study on Types 304L and 316L stainless steels.

## II. PROCEDURE

Arc-shaped fracture toughness specimens were fabricated from high-energy-rate-forged (HERF) forward-extruded cylinders and fatigue-cracked according to ASTM E399 (8). The compositions and mechanical properties of the steels are given in Table I. The material and forgings had been characterized in earlier studies (3,4) and had yield strengths ranging from 517 to 870 MPa. About half of the samples were machined with an inside radius of 6.35 mm,

* The information in this article was developed during the course of work under Contract No. DE-AC09-96SR18500 with the U. S. Department of Energy.

**TABLE 1 Heat Compositions and Forging Treatments**

| Heat[a] | Heat Compositions (wt. %) Cr | Ni | Mn | PSi | C | S | N | O (wppm) | Al |
|---|---|---|---|---|---|---|---|---|---|
| 1 | 19.2 | 7.22 | 9.23 | .014 | .41 .032 | .003 | .28 | 19 | .002 |
| 2 | 19.4 | 6.40 | 8.50 | .021 | .33 .040 | <.001 | .28 | 22 | <.001 |
| 3 | 20.1 | 6.50 | 9.10 | .019 | .59 .037 | <.001 | .29 | 10 | .001 |

[a] Heat 1 was used for forgings of nominal yield strengths of 660 and 760 MPa. Heat 2 was used for forgings of nominal yield strengths of 760 and 870 MPa. Heat 3 was used for forgings of nominal yield strengths of 930 MPa.

Forging Conditions: Extrusion die and stub punch; heat parts to 1255 K ± 10 K; hold for 10 to 15 minutes; forge 1 blow at 2 MPa ± .17 MPa; water quench; heat to 1116 K ± 10 K; forge 1 blow at 5.5 MPa ± .17 MPa; water quench.

Annealing Conditions: (Nominal Yield Strength of 517 MPa): 1114 K for 5 minutes.

an outside radius of 12.7 mm, and a thickness of 3.81 mm. The remaining samples were machined with an inside radius of 9.65 mm, an outside radius of 19.1 mm and a thickness of 5.08 mm. The crack plane was oriented normal to the circumferential direction and the direction of crack propagation was in the radial direction.

The machined specimens were exposed to tritium at 423 K with a tritium partial pressure of 4500 psi for nine months. The samples were then aged at 273 K for selected times to allow for decay to $^{3}He$ while minimizing off-gassing losses of tritium. The concentrations of tritium and $^{3}He$ were calculated from diffusivity and solubility data for hydrogen in stainless steel (3). Tritium concentrations ranged from 0-2600 atomic parts per million (appm) and helium concentrations ranged from 0-800 appm. The calculated values were checked against measured values of 3He by vacuum extraction (9). Calculated values of decay helium were about 10-15% higher than measured values due to tritium off-gassing losses during storage and handling. The samples were step-loaded at room temperature in air using a screw-driven testing machine and a crosshead speed of 8.5 x 10-3 mm /s. The load was periodically increased until cracking was detected by a drop in load or the elastic limit was reached. Once cracking initiated, the sample was held at fixed displacement and the cracking progress monitored by continuously recording the load drop until crack arrest. Cracking usually continued for three or four days. The samples were unloaded when the load drop was less than 1 kg over a three-hour period. A typical load-time record is shown in Figure 1. The samples were then heat-tinted at 623 K for 30 minutes to mark the progress of tritium-induced cracking and pulled apart. Crack lengths were measured from the heat tinted fracture surface as depicted in Figure 2. The threshold stress intensity for tritium-induced cracking was calculated from the final load and the final crack length and the stress intensity formulae for this sample geometry (8). Crack velocities during slow crack growth were determined from

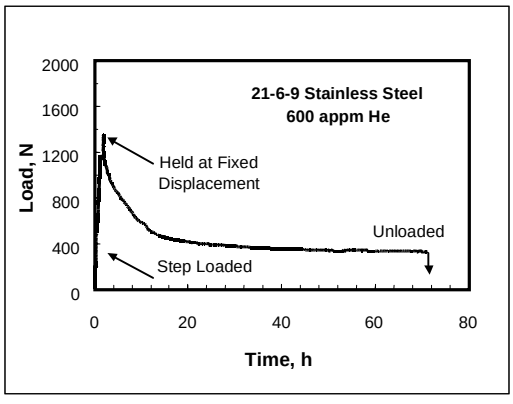


**Figure 1. Typical Load Displacement Record During Slow Crack Growth.**

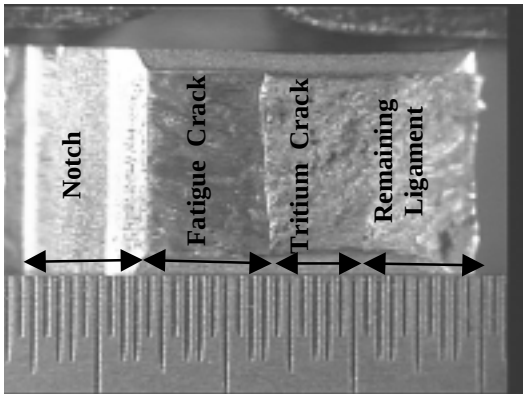


**Figure 2. Heat Tinted Fracture Surface.**

the load-time records and compliance relationships for the arc-shaped specimen.

## III. RESULTS

The results of the study are given in Figures 3-6. While unexposed samples failed by dimpled rupture (Figure 3), tritium-exposed-and-aged steels fractured by intergranular fracture (Figure 4). Thresholds for cracking decreased with increasing helium concentrations (Figure 5) while the steady state crack velocities tended to remain relatively independent of helium concentration (Figure 6).

The microstructure of these steels was typical of HERF material and consisted of patches of ~ 5 μm grains embedded in much larger, ~ 200 μm grains (7). The duplex grain size results from the onset of static recrystallization that occurs just after the final forging blow. The microstructure was approximately 15% recrystallized.

Tritium-exposed-and-aged samples were characterized by the presence of $^{3}$He bubbles, whose strain fields give rise to the black dots within the recrystallized grains (Figure 7a). Although helium bubbles measuring between 1-2 nm were homogeneously distributed throughout the grain interiors, incoherent twin boundaries and dislocations were particularly potent nucleation sites (Figures 7a and 7b). In recrystallized grains few dislocations were observed, but those that were present were "decorated" with a large number $^{3}$He bubbles.

Examination of specimens taken from the gage section (plastically strained) of tensile bars revealed differences in both $^{3}$He bubble microstructure and base microstructure when compared to the samples taken from the grips (elastically strained). In the plastically strained regions, bubbles were readily observed on the high angle grain boundaries within the "patches" of recrystallized grains (Figure 7b). These bubbles measured approximately 2.0 nm

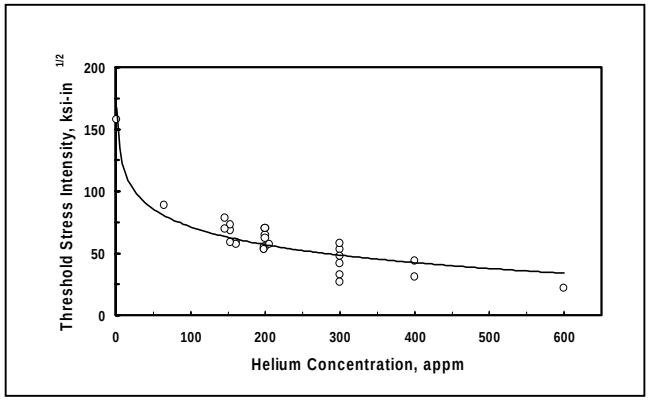


**Figure 5. Threshold Stress Intensity For Cracking For Tritium-Exposed-and-Aged 21-6-9 Stainless Steel.**

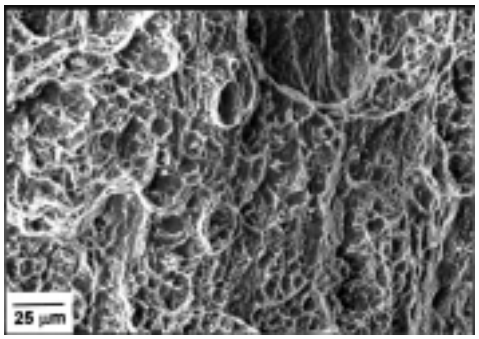


**Figure 3. Typical Dimpled Rupture Fracture Appearance For Unexposed 21-6-9 Stainless Steel.**

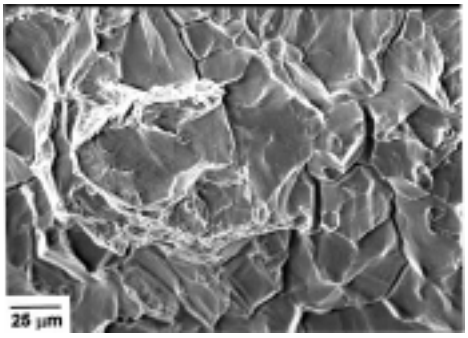


**Figure 4. Intergranular Fracture Appearance For Tritium-Exposed-and-Aged 21-6-9 Stainless Steel.**

in diameter and, in most instances, were present in large numbers. In many regions along the boundaries the bubbles appeared to have coalesced to form small cavities. Coalescence of bubbles was also observed at the incoherent twin boundaries as shown in Figure 7. The bubble distribution within the matrix appeared to remain unchanged after deformation. The coalescence of bubbles on grain and twin boundaries following plastic deformation is consistent with the intergranular fracture modes (Figure 4). Finally, in the heavily worked regions of the HERF microstructure, deformation twinning was seen instead of

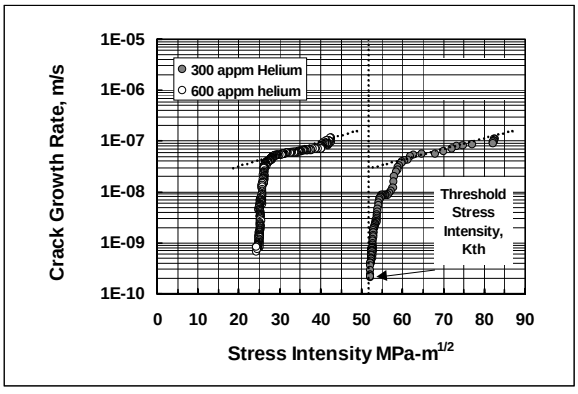


**Figure 6. Crack Velocities Versus Stress Intensity For Different Helium Concentrations.**

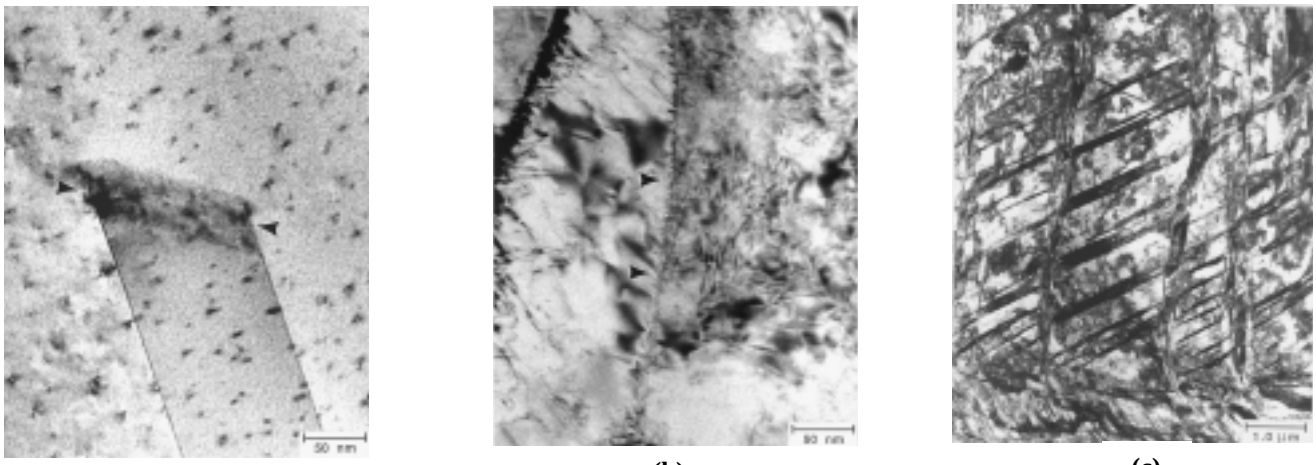

(a) (b) (c)

**Figure 7. Helium Bubble Microstructure in Tritium-Exposed-And-Aged 21-6-9 Stainless Steel: (a) Strain Fields Associated With Helium Bubbles Give Rise to the "Black Dots" In Matrix And Cluster Of Helium Bubbles At Incoherent Twin Boundary; (b) Bubbles Growth and Coalescence On A Grain Boundary; and (c) Deformation Twinning In Hardened Microstructure.**

intense plastic slip which was seen in the less worked grains (Figure 7c).

## IV. DISCUSSION

The results of this study have important implications for tritium storage vessels. First of all, the results indicate that the threshold for tritium-induced cracking depends on the age of a vessel and its exposure history to tritium. During service, the steel will age because of tritium dissolution, diffusion and decay. It will become more susceptible to delayed cracking with time. The measured relationships between cracking threshold and decay helium concentration can be used for establishing safe lifetimes for vessels in tritium service. Similar reductions in cracking thresholds by helium have been observed in Types 304L and 316L stainless steels (5).

However, there is an important difference between hydrogen induced cracking (HIC) thresholds and tritium induced cracking (TIC) thresholds in a service environment. For HIC, when the applied stress intensity exceeds the threshold for cracking a crack will grow at a rate controlled by the dissolution and diffusion of hydrogen. For TIC, the threshold for cracking depends on the helium concentration. Because of this, the helium concentration gradient in the near-surface regions of a vessel in tritium service will influence the cracking process. That is, cracks can nucleate in the heavily embrittled near surface region but cannot continue to grow because the cracking threshold is a function of the depth of penetration of the tritium during service and its decay to helium. This has been observed in vessels taken out of tritium service at the Savnnah River Site.

As the material ages and helium builds-in from tritium diffusion and decay, the material near the surface progressively weakens. When the material weakens to the point that its threshold for cracking is exceeded by the applied stresses, then a crack will nucleate or a preexisting crack will take a jump through the embrittled zone. The size of the jump will depend on the helium concentration gradient and the applied stress field. With each jump, the applied stress intensity will increase because the crack length will have increased. Freshly nucleated cracks will continue to grow in a step-wise process influenced by:

(1) Time for tritium diffusion and decay to helium;
(2) The lowering of the threshold for cracking by tritium and helium in the near surface region;
(3) Crack propagation through the embrittled zone; and,
(4) Crack arrest in the zone of material not yet penetrated by tritium.

The process repeats with the time between each successive crack jump shortened because of the increase in stress intensity associated with the longer crack.

Eventually, the crack reaches a critical size, and can continue to run through the wall controlled only by the hydrogen-induced cracking process. Hydrogen-induced cracking does not require time for the further build-in of helium from tritium decay and therefore, can occur relatively rapidly compared to the step-wise helium induced cracking described above. The details of this process are being developed into a cracking model for establishing safe lifetimes for tritium storage vessels.

Finally, when compared to earlier data for tritium-exposed-and-aged Types 316L and 304L steels (5), Type 316L stainless steel had the highest thresholds for cracking and 21-6-9 the lowest. These results are in good agreement

with those of earlier investigations by Robinson (2) and Caskey (10). In those studies, the fracture properties of both smooth and notched tritium-exposed-and-aged stainless steels decreased with increasing helium concentrations. The relative ranking of the alloys is also consistent with J-integral fracture toughness measurements similar tritium-exposed-and-aged steels (11).

The fact that 21-6-9 stainless steel was less tough than Types 304L and 316L can, in part, be explained by their yield strength differences–fracture toughness tends to decrease with increasing yield strength. However, its greater susceptibility to tritium-induced embrittlement is consistent with a fracture model described by Müllner, *et. al* (12). According to Müllner, brittle fracture will occur most easily in austenitic steels with low stacking fault energies and low densities of free dislocations. Steels with low stacking fault energies deform by twinning at lower strain levels than those with high stacking fault energies. Crack nucleation is made easier when twin lamella act as obstacles to further twin propagation. Twin lamellae are effective obstacles when the density of free dislocations is low because the high stresses at the twin-twin intersections are not be relaxed by dislocation motion.

Thus, 21-6-9 steel had the lowest fracture toughness values and would be expected to have the lowest stacking fault energy because of its lower nickel (which tends to raise the stacking fault energy) content and its higher manganese and nitrogen (which tend to lower the stacking fault energy) contents (1). The fact that Type 316L steel was not affected by tritium as much as Type 304L steel could be explained by its higher nickel content.

The effects of decay helium are also consistent with the model of Müllner because the density of free dislocations is reduced because of helium-bubble pinning. Deformation twinning occurs more easily in tritium exposed steels (Figure 7c and Reference 2). Secondly, crack nucleation is made easier because free dislocations are not available to relax the stress fields at twin-twin intersections and because of the "cohesion lowering" effects of hydrogen when it is present in the lattice.

## V. CONCLUSIONS

1. Tritium and decay helium reduced the cracking thresholds for 21-6-9 stainless steel. The threshold for cracking was dependent on the concentration of decay helium.

2. The relationship between cracking threshold and decay helium concentration coupled with a cracking model can be used for estimating the lifetime of vessels used in tritium service.

3. When compared to earlier data for tritium-exposed-and-aged Types 316L and 304L steels, Type 316L stainless steel had the highest thresholds for cracking and 21-6-9 the lowest.

4. The relative ranking of the alloys and the effects of helium are both consistent with observations that brittle fracture occurs most easily in austenitic steels with low stacking fault energies and low densities of free dislocations.

## VI. REFERENCES


1. B. C. Odegard, J. A. Brooks, and A. J. West, "The Effect of Hydrogen on the Mechanical Behavior of Nitrogen Strengthened Stainless Steel", Effect of Hydrogen on the Behavior of Materials, A. W. Thompson and I. M. Bernstein, eds., The Metallurgical Society of AIME, 1976, p. 116.

2. S. L. Robinson, "The Effects of Tritium on the Flow and Fracture of Austenitic Stainless Steels", *Hydrogen Effects. On Materiall Behavior*, N. R. Moody and A. W. Thompson, eds., TMS, Warrendale, PA, 1990, pp. 433-445.

3. G. R. Caskey, "Hydrogen Effects in Stainless Steel", *Hyd. Degradation of Ferrous Alloys*, R. A. Oriani, J. P. Hirth, M. A. Smialowski, eds., Noyes Pub., 1985, pp. 822-862.

4. M. J. Morgan, "The Effects of Hydrogen Isotopes and Helium on the Flow and Fracture Properties of 21-6-9 Stainless Steel", *Proc. Fine Symp.*, P. K. Liaw, J. R. Weertman, H. L. Marcus, and J. S. Santner, eds., TMS, Warrendale, PA, 1990, pp. 105-111.

5. M. J. Morgan and D. Lohmeier, "Threshold Stress Intensities and Crack Growth Rates In Tritium-Exposed HERF Stainless Steels", *Hyd. Eff. on Mat'l Behavior*, N. R. Moody and A. W. Thompson, eds., TMS, Warrendale, PA, 1990, pp. 459-468.

6. M. J. Morgan and M. H. Tosten, "Microstructure and Yield Strength Effects On Hydrogen and Tritium Induced Cracking In HERF Stainless Steels", *ibid.*, pp. 447-457.

7. S. L. Robinson, "Tritium and Helium Effects on Plastic Deformation in AISI 316 Stainless Steel", Materials Science and Engineering, 1987, vol. 96, p. 7.ASTM E399

8. ASTM E813-89, *Annual Book of ASTM Standards*, ASTM, Phila., PA, 1990, vol. 3.01.

9. B. M. Oliver, Rockwell International Report No. 86RC15250, Rockwell International, Rocketdyne Division, Canoga Park, CA, 1986.

10. G. R. Caskey, Jr., *Fusion Technology*, 1985, vol. 8, pp. 2293-2298.

11. P. Müllner, C. Solenthaler, P. J. Uggowitzer and M. O. Speidel, *Acta metall. mater.*, 1994, vol. 42, No. 7, pp. 2211-2217.

12. M. J. Morgan and M. H. Tosten, Tritium and Decay Helium Effects on the Fracture Toughness Properties of Types 316L, 304L and 21-6-9 Stainless Steels, Hydrogen Effects on Material Behavioir, eds., A. W. Thompson and N. R. Moody, TMS, Warrendale, PA, 1996, pp. 873-882.